

# Real-time Spatial-based Projector Resolution Enhancement

**Avery Ma\***, **Ahmed Gawish\***, **Mark Lamm\*\***,  
**Alexander Wong\***, **Paul Fieguth\***

**\*Department of Systems Design Engineering**  
**University of Waterloo**  
**Waterloo, Canada**

**\*\*Christie Digital Systems**  
**Canada Inc.**  
**Kitchener, Canada**

**Abstract** *In this paper, we present a method for real-time projector resolution enhancement. Two low-resolution sub-images are sampled from each high-resolution input image, and then pre-distorted using a spatial enhancement kernel. When the sub-images are projected with an offset, it produces an apparent high-resolution reproduction of the original image.*

**Author Keywords** projector resolution enhancement; super-resolution; Shifted Superposition; superimposed projection; point spread function; Wiener deconvolution filtering

## 1. Introduction

High-definition projection has become widely available at both consumer and enterprise levels. In the home entertainment industry, for instance, there is a strong consumer interest in 4K projectors; however, the rapid increase in the cost of higher resolution projectors is cumbersome, and hence can only be met by high-end applications such as military and large entertainment systems. As such, projector resolution enhancement techniques have received much attention both in industry and academically.

There have been a number of methods to enhance the resolution of a projector. A typical model consists of decomposing the high-resolution image to multiple low-resolution sub-images that are projected with an offset at a higher frame rate. [1, 2, 3]. The sub-images are then merged by the human visual system into a single high-resolution image that approximates the original high-resolution source. One popular approach is the multi-projector framework which involves using a combination of tiled and superimposed projectors to achieve high-resolution projection beyond the resolution limit of component projectors [4, 5]. The main issue with such multi-projector setup is that it requires careful geometric calibration and color adjustment, which make the method difficult to utilize for in practical scenarios.

To address these issues, Allen and Ulichney [6] proposed the concept of wobulation to keep the resolution enhancement system within one projector unit. In the wobulation

method, multiple low-resolution sub-images are sampled from a high-resolution source and then projected at different positions using an opto-mechanical image shifter. Based on this framework, Barshan *et al.* [7] proposed a resolution enhancement approach called Shifted Superposition (SSPOS), where a sub-image generation algorithm iteratively computes the optimized low-resolution images  $I_1$  and  $I_2$ , with one being the sub-pixel shifted version of the other. The algorithm minimizes the difference between the original high-resolution input image  $I_H$  and the simulated superimposed result  $S(I_1, I_2)$ :

$$\hat{I}_1, \hat{I}_2 = \underset{I_1, I_2}{\operatorname{argmin}} \|I_H - S(I_1, I_2)\|^2 \quad (1)$$

In traditional projection systems, it occurs that one-pixel point source from the projector does not converge into a single point after transmission through the projector-lens system. This results in blurring of the projected content, with the distortion most obvious in high-contrast regions with fine-grained details such as small font texts. As such, the perceived projection output in [7] is estimated incorporating the point spread function (PSF)  $H$  of the projector:

$$S(I_1, I_2) = I_1 * H + I_2 * H \quad (2)$$

Although the method demonstrates a substantial increase in visible high-resolution content, such sub-image generation approach is unsuitable for real-time implementation when several iterations of the algorithm are required to generate acceptable results. Additionally, the sub-image optimization is performed on an image-by-image basis, and hence the method is not generalized for video content and severe flickering artifacts can be exhibited when projecting moving texts and lines. As such, alternative projector resolution enhancement techniques that address these issues are highly desired.

In this paper, we propose a real-time spatial-based resolution enhancement approach to project high-resolution content using a low-resolution projector with an opto-mechanical image shifter. Given a high-resolution image to be displayed, we

first compute two low-resolution images that match the projector's native resolution based on the principle of SSPOS. The low-resolution sub-images are then pre-distorted prior to the projection using a spatial enhancement kernel derived based on Wiener deconvolution techniques. The proposed approach can be easily implemented in existing commercial projectors in the absence of extensive computing resources.

The rest of the paper is structured as follows. Section 2 presents the two-stage resolution enhancement approach, specifically, the sub-image generation and the derivation of the spatial enhancement kernel. The experimental results are presented in Section 3. Finally, conclusions are drawn in Section 4.

## 2. Methodology

The proposed approach effectively decomposes the iterative SSPOS approach into two separate modules: sub-image generation and pre-distortion modelling. The high-resolution input image is resampled to two low-resolution images with a half-pixel offset. Then, the low-resolution images are pre-distorted using a spatial enhancement kernel to compensate for optical aberration. The overall resolution enhancement approach consists of two modules with each serving a specific purpose and the performance of the resolution enhancement method significantly increases from one module to the next.

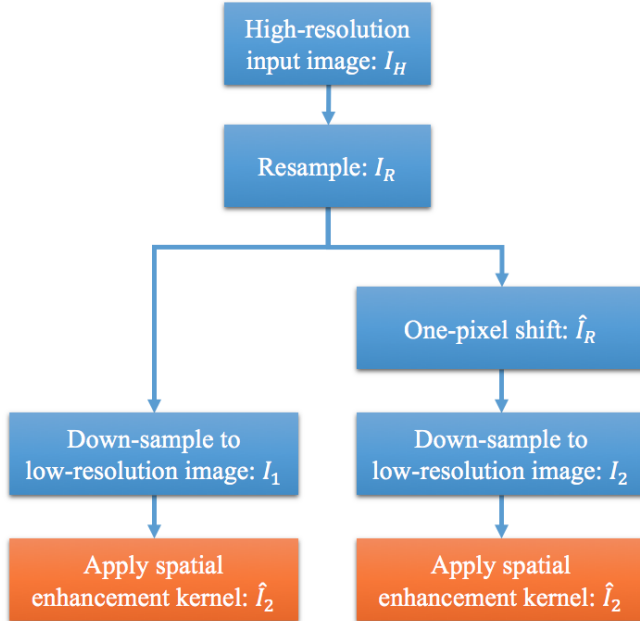


**Fig. 1:** Overview of the proposed resolution enhancement approach: Sub-image Generation (blue) and Pre-distortion Modelling (orange)

### 2.1. Sub-image Generation

In wobulation-based techniques, a half-pixel shift between the low-resolution images is widely used to produce an apparent high-resolution reproduction of the original image [3, 7, 8]. Given each high-resolution input image  $I_H$ , the objective of this stage is to generate two low-resolution sub-images  $I_1$  and  $I_2$  with a half-pixel offset. However, it is not feasible to shift an image by half of a pixel. To overcome this problem, one simple and effective solution is to convert the half-pixel shift in low-resolution images into a one-pixel shift in images with twice the resolution. As such, we first resample  $I_H$  to twice the resolution of the low-resolution image. Depending on the ratio  $r$  between the resolution of  $I_H$  and  $I_1$ , the resampled image  $I_R$  is:

$$I_R = \begin{cases} \uparrow_{\frac{r}{2}} I_H, & \text{if } r \leq 2 \\ \downarrow_{\frac{r}{2}} I_H, & \text{if } r > 2 \end{cases} \quad (3)$$

As a result of resampling, the half-pixel shift between the low-resolution images is now converted to a one-pixel shift in the resampled image. Assuming the resampled image  $I_R$  has a dimension of  $M \times N$ , the one-pixel shift operation is formulated as:

$$\hat{I}_R = \begin{pmatrix} I_R(1,1) & \cdots & I_R(1,N) & I_R(1,N) \\ I_R(2,1) & \cdots & I_R(2,N) & I_R(2,N) \\ \ddots & & \ddots & \ddots \\ I_R(M,1) & \cdots & I_R(M,N) & I_R(M,N) \\ I_R(M,1) & \cdots & I_R(M,N) & I_R(M,N) \end{pmatrix} \quad (4)$$

The two sub-images  $I_1$  and  $I_2$  are then generated by down-sampling  $I_R$  and its one-pixel shifted version  $\hat{I}_R$  to the projector's native resolution:

$$I_1 = \Downarrow_2 I_R \quad (5)$$

$$I_2 = \Downarrow_2 \hat{I}_R \quad (6)$$

In the sub-image generation stage, the resampling operation is based on *sinc* (Lanczos3) interpolation, and the down-sampling operation is based on local averaging.

### 2.2. Pre-distortion Modelling using Spatial Enhancement Kernel

In our work, we consider a spatial-based, non-iterative approach to produce optimal sub-images to compensate the optical aberration inherent in the projector-lens system. By altering the sub-frames  $I_1$  and  $I_2$  incorporating the knowledge of the PSF, the perceived image can be non-distorted when projected. The pre-distortion operation can be expressed as:

$$\hat{I}_1 = I_1 * g \quad (7)$$

$$\hat{I}_2 = I_2 * g \quad (8)$$



**Fig. 2:** The projection results as captured by a camera. For each test image, we captured the projection of the sub-images with the actuator off (left), with the actuator on (middle), and the pre-distorted sub-images with the actuator on (right)

where  $\hat{I}_1$  and  $\hat{I}_2$  are the pre-distorted sub-images. The spatial enhancement kernel  $g$  can be realized using a band-limited Wiener deconvolution filter. The derivation of the spatial enhancement kernel consists of three stages. We first measure the PSF presented in the projector-lens system. Then, a band-limited Wiener deconvolution filter is constructed using the estimated PSF. Finally, the spatial enhancement kernel is obtained from the inverse Fourier transform of the band-limited Wiener deconvolution filter.

**PSF Estimation:** The first step towards defining the spatial enhancement kernel is to measure the PSF, which represents how the projector and the optical system responds to a single-pixel projection. To accurately measure the PSF, a lens-free camera is used to capture the single-pixel response of the projector. We project a single pixel directly into the camera CMOS sensor. It is worth mentioning that this estimation is based on the assumption that the PSF is spatially invariant: the single-pixel response of the projector is uniform across the entire projected area.

**Band-limited Wiener Deconvolution Filter:** Frequency domain Wiener deconvolution filtering is widely used in image enhancement and restoration[9]. The filtering operation involves spatial-frequency domain transformations of the input image, as well as an element-by-element multiplication of the transformation result and the filter. One inevitable drawback of such technique is its computational complexity, which makes it impractical in a real-time implementation in the absence of extensive computing resources. To address this issue, we propose the use of a spatial kernel derived from the Wiener deconvolution filter. This simplifies the expensive filtering operation to merely a 2D convolution on the low-resolution sub-images. During run time, the FPGA memory fetches a part of the image with its size proportional to the size of the kernel; therefore, with a constrained kernel size, the use of

a spatial kernel can effectively reduce the amount of memory required during the real-time execution of the algorithm. To generate the spatial kernel, we first compute the Wiener deconvolution filter based on the estimated PSF and the assumption of a constant signal-to-noise ratio  $SNR$ :

$$G(u, v) = \frac{1}{H(u, v)} \left[ \frac{|H(u, v)^2|}{|H(u, v)^2| + \frac{1}{SNR}} \right] \quad (9)$$

where  $H(u, v)$  is the frequency domain representation of the PSF. The dimension of the final spatial enhancement kernel is constrained to fit in the available space and bandwidth of hardware. However, we discovered that computing the spatial kernel directly from the Wiener deconvolution filter would result in high energy terms at the center of the final spatial kernel, leading to severe over-sharpening artifacts when projecting. This was caused by the large coefficients at the high frequency components in the Wiener deconvolution filter, which we found has little or no effect to the resolution enhancement of the image. As such, we propose the use of a band-pass filter  $B(u, v)$  to attenuate the high-frequency components in the Wiener deconvolution filter prior to the spatial transformation:

$$\hat{G}(u, v) = G(u, v)B(u, v) \quad (10)$$

**Generating the Spatial Enhancement Kernel:** Based on the band-limited Wiener deconvolution filter, we first compute  $\hat{g}$ , the spatial representation of the filter by inverse Fourier transform:

$$\hat{g}(i, j) = F^{-1}[\hat{G}(u, v)] \quad (11)$$

Given a desired dimension parameter  $w > 0$  that matches the space and bandwidth of the hardware, the normalized subset of spatial enhancement kernel is formulated:

$$g(i, j) = \begin{cases} \frac{\hat{g}(i, j)}{|\hat{g}(i, j)|}, & \text{if } i \leq w \text{ and } j \leq w \\ 0, & \text{otherwise} \end{cases} \quad (12)$$

### 3. Results

In this section, we demonstrate experimental results on a prototype projector with an opto-mechanical image shifter. The system consists of a Christie Matrix StIM WQ projector (2560 x 1600) with a piezo-electric actuator introducing a sub-pixel shift in both vertical and horizontal directions. A software-triggered USB 3.0 camera is positioned about halfway between the projector and the screen to capture the superimposed projection results. Additionally, the camera is placed axially as close to the projection lens as possible to minimize keystone distortions.

In the experiment, each test image is processed, projected and captured in three different ways to demonstrate the efficacy of the proposed resolution enhancement approach. The first one is the resampled sub-images projected with the actuator off, in the projector's native resolution. The later two projections represent the resolution-enhanced results via the two modules in the proposed approach. In particular, the second one is from superimposing the sub-images with the actuator turned on to create the sub-pixel shift, and the last one is from superimposing the pre-distorted sub-images with the actuator on.

Figure 2 illustrates the difference between the three projection results on test images with different types of structural characteristics: natural images with high structural details such as brick walls and grass fields, and synthetic-looking images with high contrast details such as texts. In the first projection result with the actuator off, the projector essentially displays the sub-frames in its native resolution and the screen door artifacts remains visible between the pixels. In the second and third projection results with the actuator on, the screen door artifacts are removed and both results demonstrate a drastic increase in the apparent resolution of the projected content.

Comparing the projection results generated using the two modules in the proposed method, the resolution enhancement from the pre-distortion modelling stage can be clearly observed in synthetic regions such as small font texts. For example, circular strokes are more identifiable for letters such as 'a' and 'e'. Whereas on natural images, from a distance the enhancement from the pre-distorted sub-frames is hard to notice, but upon close inspection it is clear that there is a significant resolution enhancement in regions of the image with fine-grained details, such as the ocean waves, the wheels of the bicycle, and the bricks on the wall. In future work, it may be interesting to incorporate the underlying characteristics of the image into generating multiple enhancement kernels that are most suitable for particular types of content.

Finally, the proposed resolution enhancement approach was implemented at 4K resolution and 60Hz, meaning the projection system receives 4K high-resolution images and projects resolution-enhanced images with 1/2 the pixels in a 4k image. The approach was tested using a Xilinx Kintex-7 7K160 FPGA, which is the second smallest FPGA in the Kintex-7

family. It was shown that the proposed pipeline can easily fit within the existing image processing architecture, taking only a minor portion of the available space and bandwidth.

### 4. Conclusions

In this work, we present a real-time resolution enhancement method for projectors. For each high-resolution input image, the proposed method generates two pre-distorted sub-images at projector's native resolution. By projecting with a half-pixel offset, the proposed approach can extend the resolution of the projector beyond its original capability. Most importantly, the proposed resolution enhancement method can be easily implemented using low-cost FPGA hardware, which can potentially lead to the wide adoption of this technology in commercial projectors.

### 5. Acknowledgments

This work was supported by the Natural Sciences and Engineering Research Council of Canada, Canada Research Chairs Program, and the Ontario Ministry of Research and Innovation.

### 6. References

- [1] P. Didyk, E. Eisemann, T. Ritschel, K. Myszkowski, H.-P. Seidel, Apparent display resolution enhancement for moving images, *ACM Transactions on Graphics (TOG)* 29 (4) (2010) 113.
- [2] F. Berthouzoz, R. Fattal, Apparent resolution enhancement for motion videos, in: *Proceedings of the ACM Symposium on Applied Perception*, ACM, 2012, pp. 91–98.
- [3] A. Said, Analysis of subframe generation for superimposed images, in: *Image Processing, 2006 IEEE International Conference on*, IEEE, 2006, pp. 401–404.
- [4] N. Damera-Venkata, N. L. Chang, Realizing super-resolution with superimposed projection, in: *Computer Vision and Pattern Recognition, 2007. CVPR'07. IEEE Conference on*, IEEE, 2007, pp. 1–8.
- [5] C. Jaynes, D. Ramakrishnan, Super-resolution composition in multi-projector displays, in: *IEEE Int'l Workshop on Projector-Camera Systems*, Vol. 8, 2003.
- [6] W. Allen, R. Ulichney, 47.4: Invited paper: Wobulation: Doubling the addressed resolution of projection displays, in: *SID Symposium Digest of Technical Papers*, Vol. 36, Wiley Online Library, 2005, pp. 1514–1517.
- [7] E. Barshan, M. Lamm, C. Scharfenberger, P. Fieguth, 35.3: Resolution enhancement based on shifted superposition, in: *SID Symposium Digest of Technical Papers*, Vol. 46, Wiley Online Library, 2015, pp. 514–517.
- [8] B. Sajadi, M. Gopi, A. Majumder, Edge-guided resolution enhancement in projectors via optical pixel sharing, *ACM Transactions on Graphics (TOG)* 31 (4) (2012) 79.
- [9] R. C. Gonzalez, R. E. Woods, *Digital Image Processing* (3rd ED), Prentice-Hall, Inc., Upper Saddle River, NJ, USA, 2006.